

2010

# Strial capillary permeability following noise exposure in mice

Noel Y. Dwyer

Follow this and additional works at: [http://digitalcommons.wustl.edu/pacs\\_capstones](http://digitalcommons.wustl.edu/pacs_capstones)



Part of the [Medicine and Health Sciences Commons](#)

---

## Recommended Citation

Dwyer, Noel Y., "Strial capillary permeability following noise exposure in mice" (2010). *Independent Studies and Capstones*. Paper 611. Program in Audiology and Communication Sciences, Washington University School of Medicine. [http://digitalcommons.wustl.edu/pacs\\_capstones/611](http://digitalcommons.wustl.edu/pacs_capstones/611)

This Thesis is brought to you for free and open access by the Program in Audiology and Communication Sciences at Digital Commons@Becker. It has been accepted for inclusion in Independent Studies and Capstones by an authorized administrator of Digital Commons@Becker. For more information, please contact [engeszer@wustl.edu](mailto:engeszer@wustl.edu).

**STRIAL CAPILLARY PERMEABILITY FOLLOWING NOISE  
EXPOSURE IN MICE**

**by**

**Noël Y. Dwyer**

**A Capstone Project  
submitted in partial fulfillment of the  
requirements for the degree of:**

**Doctor of Audiology**

**Washington University School of Medicine  
Program in Audiology and Communication Sciences**

**May 20, 2011**

**Approved by:**

**Kevin K. Ohlemiller, Ph.D., Capstone Project Advisor  
Brian Faddis, Ph.D., Secondary Reader  
Keiko Hirose, M.D., Secondary Reader**

***Abstract:** A study of strial capillary permeability using fluorescent microspheres and immunohistochemistry in mice that do or do not exhibit a reduction in endocochlear potential following a single, intense noise exposure.*

copyright by

Noël Y. Dwyer

2011

## **ACKNOWLEDGMENTS**

Many thanks to Kevin Ohlemiller, Ph.D., Patty Gagnon, M.S. and Angie Schrader.

Thanks also to Keiko Hirose, M.D. and Brian Faddis, Ph.D.

**TABLE OF CONTENTS**

Acknowledgments ..... (ii)

Table of Contents ..... (1)

List of Images ..... (2)

Abbreviations ..... (3)

Introduction ..... (6)

Methods ..... (17)

Results ..... (19)

Discussion ..... (31)

References ..... (35)

**LIST OF FIGURES**

Figure 1	
Basic structure of scala media .....	(7)
Figure 2a	
Cell layers of stria vascularis .....	(8)
Figure 2b	
Pumping mechanisms of the stria vascularis .....	(9)
Figure 3	
Tight junctions of the marginal and basal cell .....	(11)
Figure 4	
Strial capillary endothelial cell transmembrane transport .....	(12)
Figure 5	
Proposed breach of strial endothelial capillary wall .....	(12)
Figure 6	
Basal turn EP in CBA/J and B6.CAST mice .....	(13)
Figure 7	
Cochlear lateral wall pathology in noise exposed CBA and B6.CAST mice.....	(14)
Figure 8	
1.0 and 0.5 $\mu\text{m}$ bead dispersion in CBA/J control and noise exposed mice .....	(20)
Figure 9	
0.5 and 0.2 $\mu\text{m}$ bead dispersion in CBA/CaJ control and noise exposed mice .....	(21)
Figure 10	
0.5 $\mu\text{m}$ and 0.02 $\mu\text{m}$ bead dispersion in BALB and CBA/J control and noise exposed mice ...	(22)
Figure 11	
0.2 and 0.02 $\mu\text{m}$ bead dispersion in B6 and CBA control and B6 noise exposed mice .....	(23)
Figure 12	
1.0, 0.2 and 0.02 $\mu\text{m}$ bead dispersion in CBA/CaJ control mice .....	(23)
Figure 13	
IgG results for B6, BALB and CBA control and noise exposed mice .....	(26)
Figure 14	
IgG in CBA/CaJ control and noise exposed mice at 40x and 60x objectives .....	(26)

Figure 15a  
IgG in B6 control and noise exposed mice, 40x objective ..... (27)

Figure 15b  
IgG in B6 control and noise exposed mice, 60x objective ..... (28)

Figure 16a  
IgG in BALB control and noise exposed mice, 40x objective ..... (29)

Figure 16b  
IgG in BALB control and noise exposed mice, 60x objective ..... (30)

## ABBREVIATIONS

Ab – antibody

B6 – C57BL/6J

BALB – Balb/cJ

BC – basal cells

CBA – CBA/CaJ

dB – decibel

EP – endocochlear or endolymphatic potential

ES – endolymphatic space

GJ – gap junction

HRP – horseradish peroxidase

IC – intermediate cells

IgG – immunoglobulin G

IHC – inner hair cell

IS – intrastrial

ISP – intrastrial potential

K<sup>+</sup> – potassium ion

MC – marginal cells

mL – milliliter

Na<sup>+</sup> – sodium ion

NE – noise exposure

OC – organ of Corti

OHC – outer hair cell



PBS – phosphate buffer saline, ph 7.4

RL – reticular lamina

RM – Reissner's membrane

sc – scala

SNHL – sensorineural hearing loss

SPL – sound pressure level

spL – spiral limbus

spLig – spiral ligament

stC – stereocilia

stV – stria vascularis

TJ – tight junction

TRP – transient receptor potential

## 1. Introduction

From a numerical perspective, the human ear can respond to frequencies between 20 and 20,000 Hz; and the range of hearing extends from 0 to 140 dB SPL (Clark and Ohlemiller, 2008; Robles and Ruggero, 2001). The ability of the ear to resolve wide ranges of frequency and intensity is achieved through a combination of processes: passive mechanics of the basilar membrane, active mechanics derived from outer hair cell (OHC) motility and mechano-electrical transduction, or stereocilia transduction and ion channel activation. It is stereocilia transduction or neural transduction that is ultimately responsible for the system's ability to operate at extremely high speeds. Transduction refers to the transformation of mechanical energy into a biochemical neural code, which is initiated by shearing of the hair cell stereocilia and subsequent opening (or closing) of ion channels. An ion-gating mechanism is located on stereocilia, which are connected by tip links. It is the tension on these tip links caused by deflection of stereocilia that is thought to 'pull open' the ion channels and allow for the influx of potassium ions ( $K^+$ ) from the endolymphatic space (ES) into the hair cell, depolarizing it (Ohmori, 1992; Hudspeth et al., 2000). While the specific gating molecule, believed to be in the superfamily of transient receptor proteins (TRPs), has been debated (Kwan et al., 2006), the mechanics involved have been compared to that of a trapdoor, suggesting more of a physical rather than ion-mediated gate due to the sheer speed of its operation.

The cochlear duct is fluid-filled: scala tympani and scala vestibuli contain perilymph, and scala media contains endolymph. The different concentrations of the constituents comprising these extracellular fluids provide the electrochemical gradients required for hair cell transduction current. Depolarization of the hair cell and the rapid influx of  $K^+$  ions from the ES rely on two gradients in scala media: a voltage gradient and a concentration gradient. Perilymph has a low

concentration of  $K^+$  ions, a high concentration of  $Na^+$  ions and a low positive charge ( $\sim 0$  mV in scala tympani,  $\sim 2-5$  mV in scala vestibuli). Endolymph is characterized by a high  $K^+$ , low  $Na^+$  concentration and a *high* positive charge of 80-100 mV (depending on species) termed the endocochlear potential (EP) (Takeuchi et al., 2001; Wangemann, 2006). The electrical gradient driving ions into hair cells is further increased by the hair cell intracellular potential ( $\sim -40$  mV) (Dallos, 1986, as cited in Gelfand, 2007). The overall gradient established by the difference in voltage is therefore approximately 120-160 mV, the largest trans-epithelial voltage in the body (Wangemann, 2006; Hibino and Kurachi, 2006; Yost, 2000). It is the EP that drives sensory transduction; it is responsible for the high sensitivity of hair cells to mechanical stimulation, and it is essential for hearing (Hibino and Kurachi, 2006; Takeuchi et al., 2001). The high  $K^+$  concentration of scala media and the EP are generated by the stria vascularis (stV) and rely on  $K^+$  cycling and strict separation of high- and low- $K^+$  cochlear fluids.

### *1.1 Anatomy and Physiology of the Cochlear Lateral Wall*

The lateral wall is comprised of the spiral ligament (spLig) and the stria vascularis (Fig. 1). Stria vascularis is medial to spLig and faces the ES. Spiral ligament contains five types of fibrocytes (I-V), all of which are surrounded by perilymph and communicate using gap junctions (GJs). The stria vascularis is a highly vascularized epithelium composed of three cell types: marginal cells (MC), intermediate cells (IC) and basal cells (BC); each layer of cells perform specific functions necessary to generate and maintain the EP (Fig.2a). Marginal cells have direct contact with the ES and are joined by tight junctions (TJs).

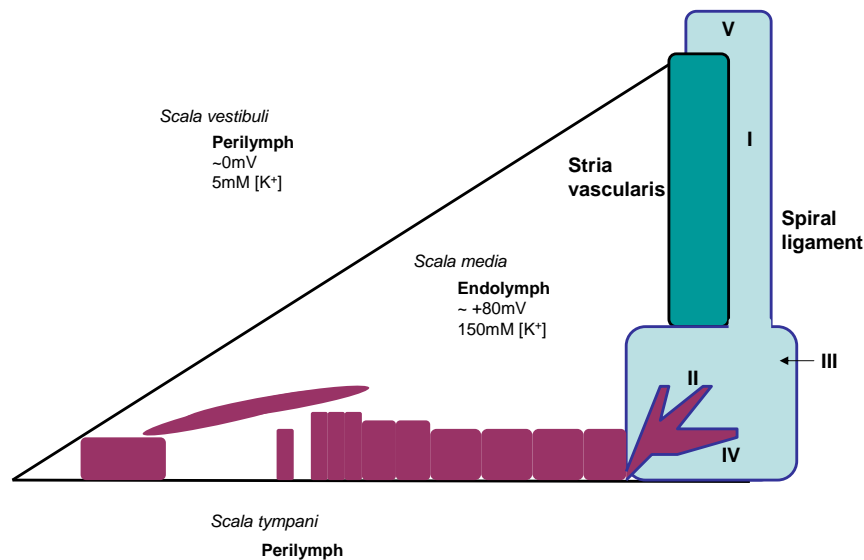


**Fig.1** Basic structure of scala media and the lateral wall. Spiral ligament is composed of fibrocytes (Types I-V) joined together by gap junctions; outer sulcus cells enter spiral ligament basally as digitated processes. Marginal cells of the stria vascularis face the endolymphatic space; and basal cells of the stria communicate with fibrocytes via gap junctions.

MCs are thought to be responsible for  $K^+$  secretion into endolymph through specific ion transport mechanisms (Wangemann, 2002; Hibino and Kurachi, 2006). ICs are connected by GJs and appose the lateral-most cell layer of BCs (also connected via GJs to one another and ICs). Given this communication between ICs and BCs, these two layers are sometimes considered functionally one. Basal cells also connect via GJ to fibrocytes of the spLig. It is hypothesized that  $K^+$  enters stV from spLig through a complex of GJs that starts with Type II fibrocytes in spLig, then via channels are taken up by BCs and then move into ICs (Wangemann, 2002; Hibino and Kurachi, 2006). Intermediate cells release  $K^+$  ions into the intrastrial space, where it is then taken up by MCs and pumped back into the endolymph in the ES (Wangemann, 2002). The intrastrial space is crucial because its charge of  $\sim 90 - 100$  mV is similar to the EP but with a low concentration of  $K^+$ , meaning the IC is the primary layer responsible for generating the high  $K^+$  in endolymph and thus the high EP (Wangemann, 2002; Hibino and Kurachi, 2006). Significant to this study is that the strial capillary network runs directly through the intrastrial space. Capillary endothelial cells are connected by essentially ion-tight junctions that maintain (Suzuki et al, 1998). This ‘blood-labyrinth barrier’ (keeping blood separate from fluid of the

intrastrial space) could break down as a result of intense noise exposure. Subsequent leakage would cause dissipation of the  $K^+$  ions and thus reduce or abolish the EP.

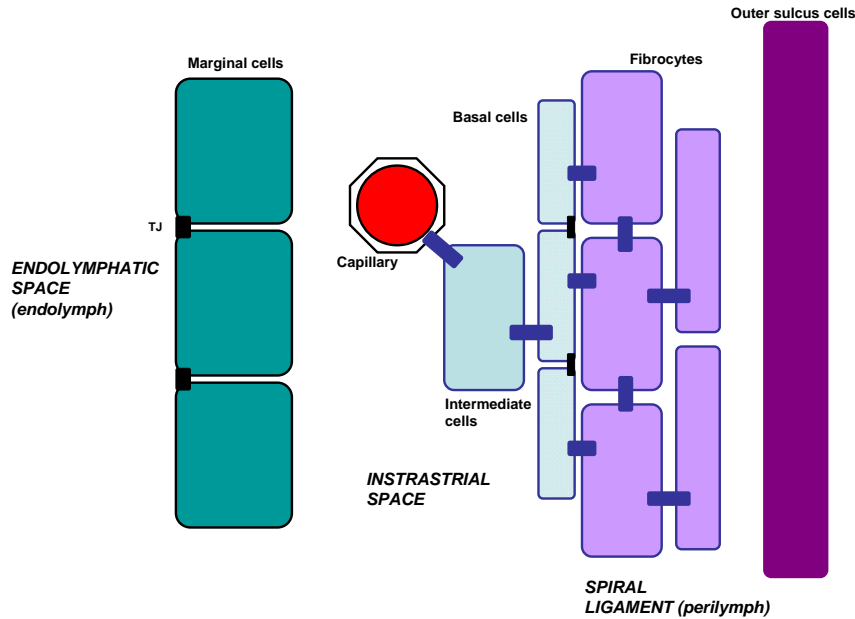


**Fig. 2a** Basic schematic of the 3 cell layers of stria vascularis; marginal cells abut the endolymphatic space and are joined by tight junctions (TJ); intermediate and basal cells communicate with one another and with fibrocytes of spiral ligament via gap junctions (GJ), but basal cells themselves are joined by TJs;  $K^+$  ions cycling through outer sulcus cells are taken up from perilymph by fibrocytes and then on to the stria vascularis.

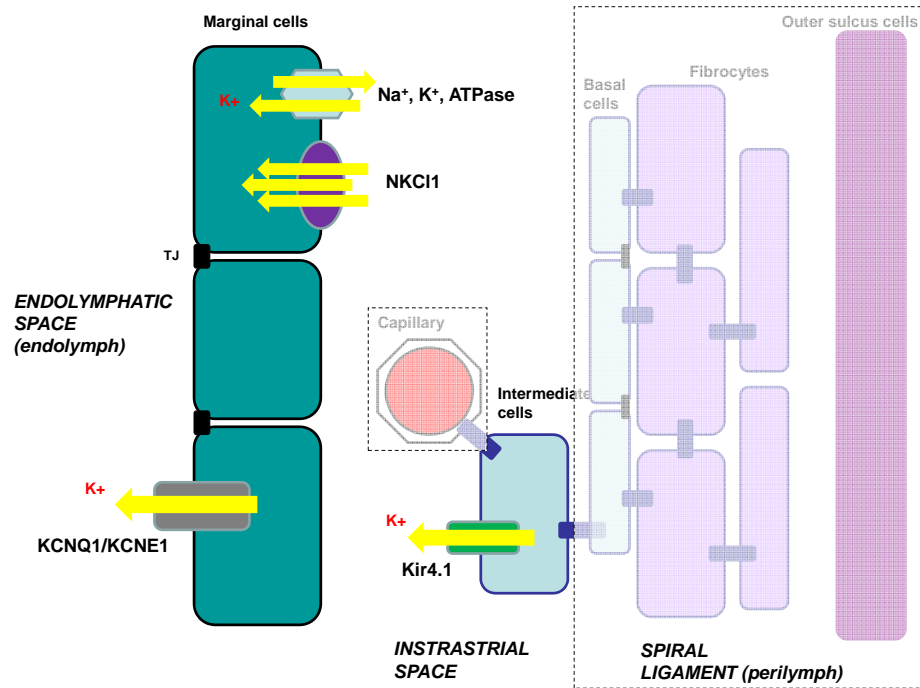


**Fig 2b** Schematic showing the primary pumping mechanisms in the stria vascularis; the barrier between endolymph and stV is formed by marginal cell tight junctions, which are ion-tight. The EP is generated across basal cells, connected to ICs via gap junctions; ICs pump  $K^+$  ions into the intrastrial space, which are then taken up by MCs before being secreted into the endolymphatic space. Loss of these ion-tight junctions could result in dissipation of  $K^+$  ions and loss or reduction of the EP.

## 1.2 Cochlear Compartments and $K^+$ Cycling

To perform its essential function, the stria is faced with the task of moving  $K^+$  up both its chemical and electrical gradients, which is in part accomplished by active and passive  $K^+$  current loops in the cochlea (Hibino and Kurachi, 2006; Wangemann, 2002). Although the number of loops and structures involved has been an intensely researched area, it is generally accepted that the primary loop is the recycling of  $K^+$  ions from perilymph. through the lateral wall first fibrocytes of the spiral ligament, then through gap junctions in the basal and intermediate cell layers and then pumped back into the ES (Hibino and Kurachi, 2006; Wangemann, 2002, 2006; Nin et al., 2008). Wangemann (2002) proposes two additional current loops: a path from the ES back into spLig fibrocytes and then cells of the stV and a path from the ES across RM into spLig and then on to stV. Significantly, while the exact pathways of the  $K^+$  cycle are still being investigated, all three loops convene in spLig, where  $K^+$  ions are pumped into stV and then from stV into the ES. Fundamental to the operations of these pathways is compartmental integrity. Any breach in compartmental boundaries could result in excessive leakage of  $K^+$  and EP dissipation. Endolymph in the ES is confined by three tissues whose cells are joined by TJs: Reissner's membrane, the reticular lamina (RL), and marginal cells of the stria vascularis. While there is little research directly addressing possible pathological responses to noise on RM integrity, there is evidence that noise can damage structures of the RL. Ahmad and colleagues (2003) observed acute changes in the EP (depressed EP) following noise exposure, attributed to OHC focal lesions and damage to sensory and supporting cells, i.e. temporary disruption of the RL. However, chinchillas were used as subjects, and the same phenomenon has yet to be proven to represent a general mammalian phenomenon.

### 1.3 *Metabolic and structural requirements of EP generation*

We may consider that normal EP generation posed two requirements. The first is metabolic. To support the high metabolic demands of transduction, the stria vascularis is fed by a rich, complex network of capillaries located in the intrastrial space (i.e. between marginal and intermediate cells). Any mismatch between  $K^+$  'sinking' by the organ of Corti and  $K^+$  movement by the stria will therefore lead to EP reduction. As we will see, this may occur during loud noise exposure. The second requirement is spatial integrity: One moved energetically 'uphill' by the stria,  $K^+$  cannot be allowed to passively redistribute in the ligament or across the ion-tight boundaries of scala media. Ion boundaries that could potentially be rendered abnormally 'leaky' under pathologic circumstances include the reticular lamina, and Reissner's membrane. They also include boundaries within the stria itself. The intrastrial space, bounded by marginal cells medially and basal cells laterally (Fig. 2b) is ion-tight, and it is this space from which  $K^+$  is moved into strial marginal cells by the Na.K-ATPase and Na/K/Cl co-transporting pumps. Should the tight junctions between marginal or basal cells be disrupted, we would expect the EP to decline (Fig.3).

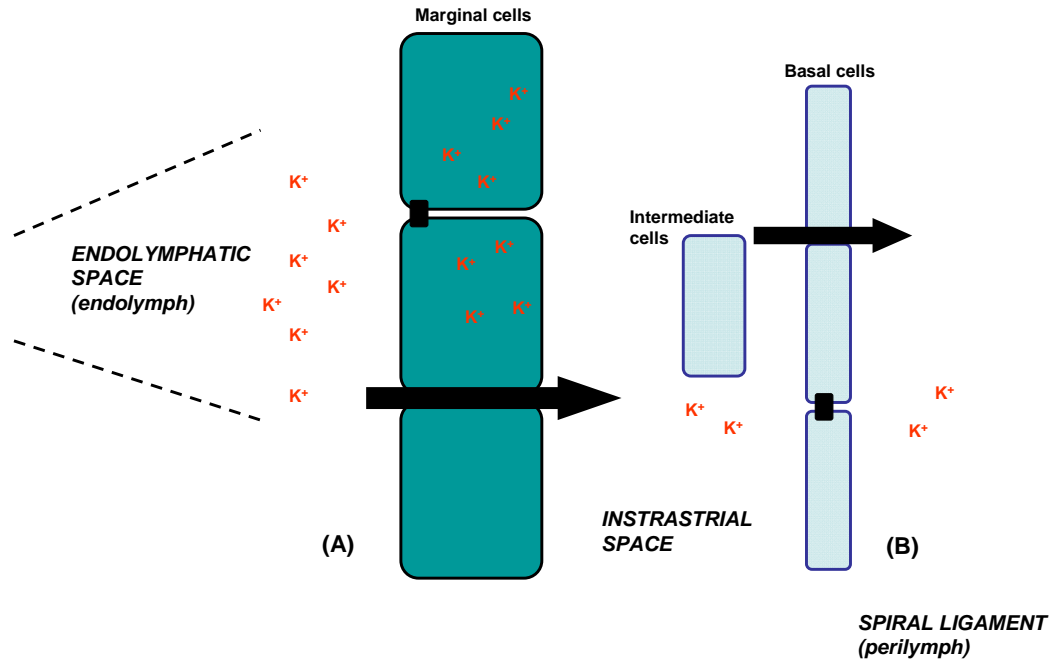


**Fig. 3** Schematic showing how breakdown of tight junctions (in black) of marginal cells (A) or basal cells (B) could lead to the dissipation of  $K^+$  and reduction of the EP. Potassium ion concentration is high in the endolymphatic space and in the marginal cells and low in the intrastrial space and spiral ligament. Because of normally present ionic gradient, loss of tight junctions would result in passive  $K^+$  movement out of the endolymphatic space, disrupting the EP.

In addition, presumably there exists a steep  $K^+$  gradient across the walls of strial capillaries.

Although this has not been explicitly demonstrated, significant abnormal permeability of strial capillaries could also act to dissipate intrastrial  $K^+$  levels. Transport of metabolites across strial capillaries is highly regulated, and relies principally on active endothelial cell mechanisms. To prevent unregulated metabolite and ion movement, capillary endothelial cells are joined by tight junctions. Noise or other stress could rupture these junctions, allowing  $K^+$  to equilibrate across capillary walls (Figs.4, 5).



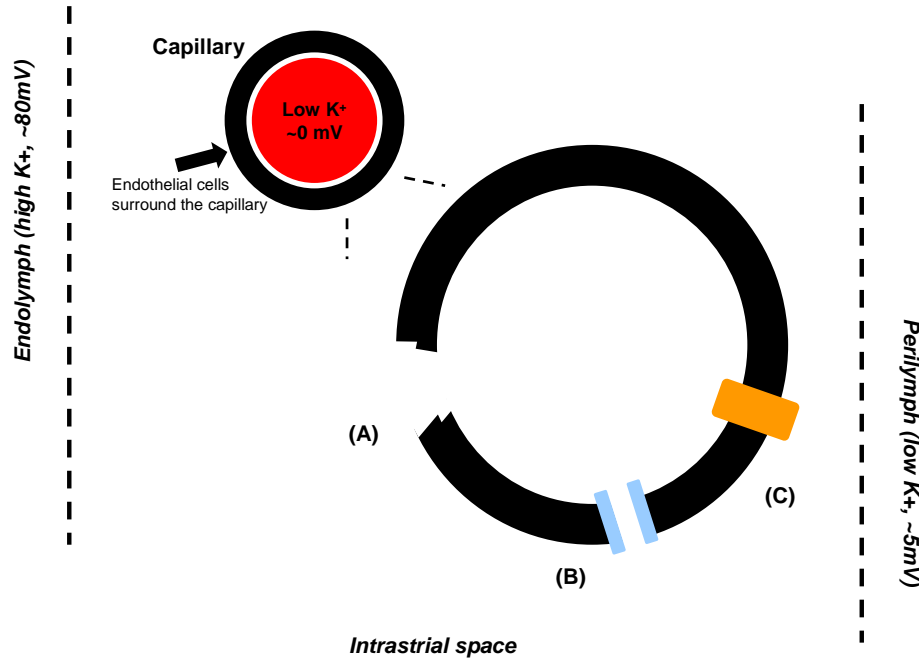


**Fig. 4** Illustration of strial capillary endothelial cell transmembrane transport (A-C); (A) unnatural capillary permeability resulting from intense noise exposure; a breach in endothelial cell TJs could lead to K<sup>+</sup> dissipation, evidenced by excessive leakage into the peri-capillary/intrastrial spaces; (B-C) illustrate normal transport mechanisms (pores or transmembrane proteins, respectively).

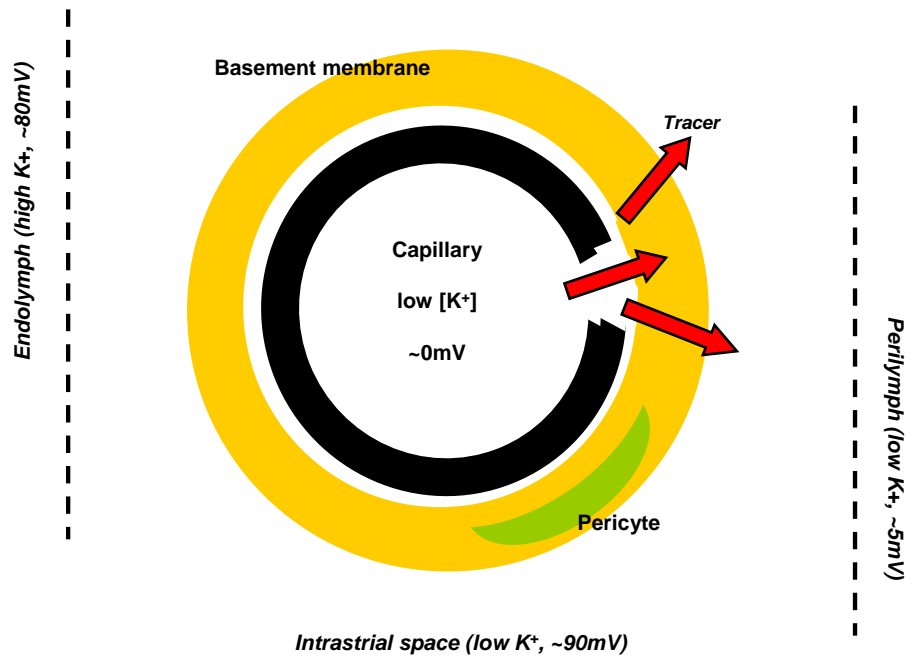


**Fig. 5** Loss of capillary integrity would be expected to take the form of excessive leakage of a tracer (in this case fluorescent beads and IgG and albumin); additionally, any breach of tight junction could result in disruption of potassium concentration in the intrastrial space due to the difference in charge of the intrastrial fluid and within the capillary; disruption of K<sup>+</sup> ions could lead to reduction or abolishment of the EP.

Supporting this model, Lin and Trune (1997) evaluated disruption of the blood-labyrinth barrier in the stV in the C3H/*lpr* autoimmune mouse model. Their results indicated a breakdown of capillary TJs in the stV evidenced by vessel leakage. In addition, mice that lack the gap junction (GJ) protein connexin30 (*Cx30*<sup>-/-</sup>) fail to produce an EP, which results in hearing impairment.

Using Cx30<sup>-/-</sup> mice, work by Cohen-Salmon et al. (2007) found disruption of the intrastrial fluid-blood barrier resulting from this connexin30 deficiency, accounting for the absence of an EP.

#### 1.4 Effects of noise on the EP and cochlear lateral wall

Although research showing cochlear lateral wall damage by noise has a long history (Wang et al., 2002; Hirose et al., 2005) only recently has quantitative work tied specific stria injury to measured EP reduction (Hirose and Liberman, 2003; Ohlemiller and Gagnon, 2007). Following a single intense exposure (2 hr, 112-116 dB SPL, 8-16 kHz) acute changes to spLig included degeneration of type II fibrocytes and stria swelling, the chronic effects of which extended to significant loss of type II fibrocytes and stria breakdown of MCs and ICs, particularly reduced membrane surface area, which is expected to decrease ion transport efficiency (Hirose and Liberman, 2003). Hirose and colleagues also importantly distinguished between EP reduction caused by rupture of the reticular lamina and EP reduction associated with lateral wall pathology that does not clearly violate ion-tight boundaries.

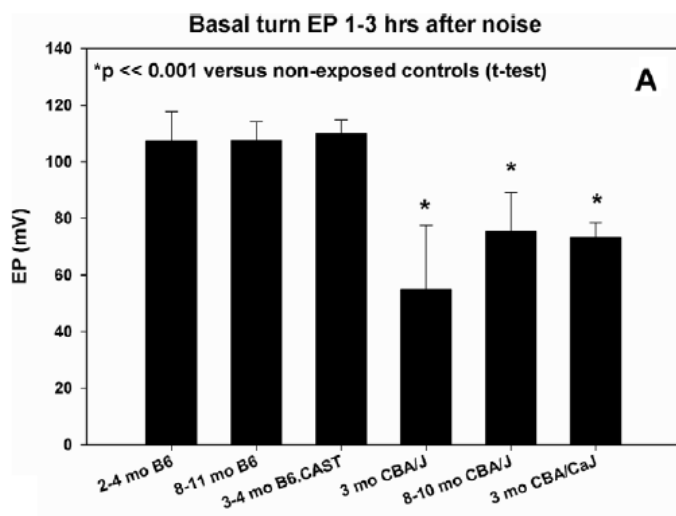


**Fig. 6** Basal turn endocochlear potential (EP) in young and old B6 mice and CBA/J mice following noise exposure. 1-3 hours after a single intense noise exposure the EP was significantly reduced in CBA-related mice but not in B6-related strains (From Ohlemiller and Gagnon, 2007).

The work of Hirose and colleagues was conducted in CBA/CaJ mice, a popular ‘good hearing’ inbred mouse strain. Ohlemiller and Gagnon (2007) confirmed and extended this work,

further showing that, for a similar exposure, whether EP reduction and measurable lateral wall injury occur depends on mouse strain—that is, on the genetic background. By contrast with CBA/J and CBA/CaJ mice, in the hours after a single severe noise exposure C57BL/6-related mice show neither EP decline (Fig.6) or measureable injury to the cochlear lateral wall (Fig. 7). A third inbred strain (BALB/c) showed noise characteristics similar to CBA. The existence of strains that do, or do not exhibit EP reduction after noise provides an opportunity to test its cellular and biochemical requirements. Since rupture of the reticular lamina could be ruled out as a necessary condition for EP reduction in both strains, these findings collectively point to genetically-modifiable events within the lateral wall itself. These events remain unknown. However, the identification of two mouse strains that differ qualitatively in their response to the same noise exposure permits us to use these strains to identify the proximate causes of EP reduction.

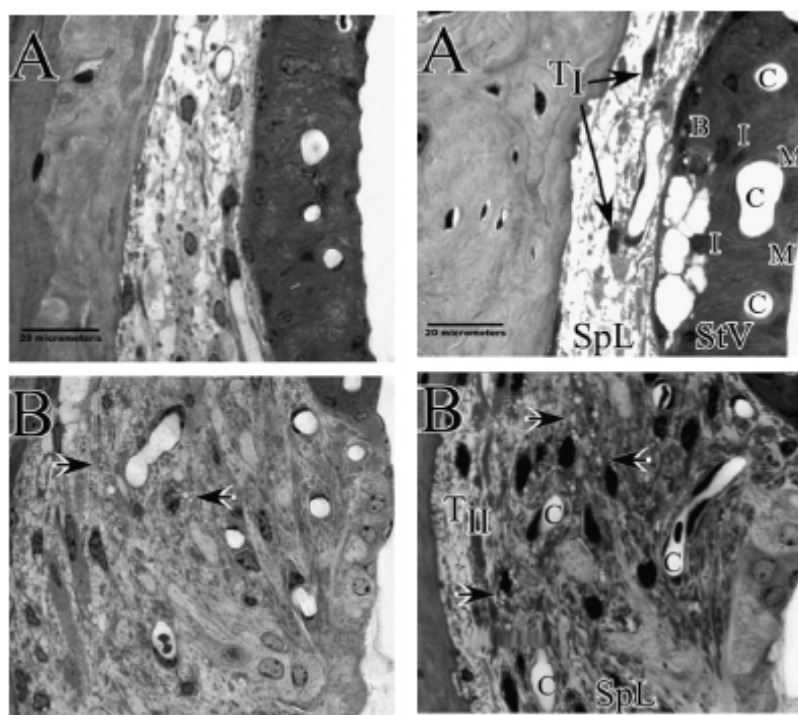


**Fig. 7 (Left column)** Cochlear upper basal turn lateral wall and spiral limbus in CBA/J mouse 1-3 h after noise. Acute stage following noise exposure CBA mice shows (A) shrinking of Type I fibrocytes (arrows) and vacuolized basal cells (BC) within the stV; (B) Type II fibrocytes in spLig appear to have vacuoles (arrows); **(Right column)** Cochlear upper basal turn, lateral wall and spiral limbus in B6.CAST mouse 1-3 h after noise. Comparison of the same cells and regions as shown for the CBA shows little injury to the major affected cells types; TI and TII: Type I and II fibrocytes; SpL: spiral ligament; StV: stria vascularis; BC: basal cell layer; IC: intermediate cell layer; MC: marginal cell layer; C: capillary. (From Ohlemiller and Gagnon, 2007).

### 1.5 Purpose of the present study

Both strial basal cell anomalies and the abnormalities within spiral ligament suggest abnormal buildup of  $K^+$  ‘upstream’ of the strial middle cell layers, so that the primary pathology probably occurs within the stria. Two major classes of events can be posited to underlie noise-related EP reduction in CBA mice. The first encompasses metabolic events, such as reduced marginal cell function. The second posits a breach of compartmental integrity, either within the stria itself, or of the stria as a whole. If for example, noise were to promote abnormally leaky strial capillaries, critical  $K^+$  gradients could be dissipated across capillary walls. Alternatively, breach of the tight junctions that lie at the boundaries of the stria could dissipate required high  $K^+$  levels within the stria. The vacuolization of strial basal cells, combined with apparent shrinkage of Type I fibrocytes in the ligament are consistent with the latter interpretation. The purpose of this study is to investigate whether noise-related EP reduction in CBA/J and CBA/CaJ mice (collectively CBA) and BALB/cJ (BALB) mice results from either occlusion or excessive permeability of strial (primarily) or potentially ligament capillaries. Both capillary occlusion and abnormal permeability were probed by application of fluorescent beads of varying sizes at the time of sacrifice and by immunohistochemistry, utilizing albumin and immunoglobulin G (IgG) to identify possible excessive leakage. Subjects were noise-exposed and non-exposed CBA, BALB and B6 mice. Evidence for capillary occlusion following a single intense noise exposure in CBA and/or BALB mice is expected to take the form of exclusion of fluorescent beads *larger* than the occluded vessel. Evidence for capillary leakage is expected to take the form of dispersion into the pericapillary space of smaller fluorescent beads as well as albumin and IgG. This study is one of the first to test a direct association between microvascular effects of noise and reduction of the EP.

## 2. Methods

### 2.1. *Animals*

All procedures were approved by the Washington University Institutional Animal Care and Use Committee. CBA/CaJ, CBA/J, C57BL/6J, and BALB/cJ mice were raised in the Washington University/CID animal facility, and were derived from breeders originally purchased from the Jackson Laboratory. Five mice per strain per condition were included in this study. Selection was sex-independent, and all animals (control and noise-exposed) were between 2 and 5 months of age at the time noise exposure and either fluorescent bead perfusion or immunohistochemistry.

### 2.2. *Noise Exposure*

Noise exposure was performed in a foam-lined, double-walled soundproof room (Industrial Acoustics). Animals were placed in a rotating wire cage surrounded by four speakers. Broadband noise was band-passed at 4.0-45.0 kHz; and animals were exposed in twos or threes at 110 dB SPL for two hours. Following exposure mice were sacrificed for either fluorescent bead perfusion or immunohistochemistry.

### 2.3 *Fluorescent Microspheres*

At the end of the exposure, animals were overdosed with sodium pentobarbital. With the abdominal aorta clamped, animals were perfused transcardially with 0.1M PBS (pH 7.4). This was immediately followed by 3mL of fluorescent microspheres of two sizes (0.02  $\mu\text{m}$  and 0.5  $\mu\text{m}$ , at a 1:1 ratio; FluoSpheres® Invitrogen, Molecular Probes. cat #s F8812 and F8787 respectively). Microspheres were sonicated for 1 minute prior to perfusion. Cochleae were then

harvested and immersed in 4% paraformaldehyde. The stapes was removed and a small hole was made in the apex of the cochlear capsule. Complete infiltration of the cochlea by fixative was achieved by gently manipulating a transfer pipet. Cochleae were fixed overnight in 4% paraformaldehyde, decalcified in sodium EDTA for 72h and cryopreserved per Whitlon, Szakaly and Greiner (2001). Cochleae were sectioned at 100 $\mu$ m, dried overnight in darkness, then coverslipped with Fluoromount G (SouthernBiotech, cat # 0100-01) for imaging.

#### 2.4. *Immunohistochemistry*

At the end of the noise exposure animals were overdosed and with the abdominal aorta clamped perfused transcardially with 4% paraformaldehyde. Cochleae were harvested and immersed in the same fixative where the stapes was removed, an apical hole was made, and complete infiltration of fixative was achieved using a transfer pipet. Cochleae remained in the same fixative for 1 hour (Cohen-Salmon et al, 2007) and then were decalcified in sodium EDTA for 72h, followed by cryopreservation per Whitlon, Szakaly and Greiner (2001). Cochleae were sectioned at 8 $\mu$ m for immunohistochemistry using either albumin or immunoglobulin G (IgG) (Cohen-Salmon et al., 2007; Trune, 1997).

#### *IgG*

Slides were washed three times in 0.1M PBS (pH 7.4), permeabilized with 0.1% Triton-X 100 (Sigma), then incubated for 1hr at room temperature with the primary antibody (Alexa Fluor® 488 goat anti-mouse IgG (H+L) IgG, Invitrogen™, cat # A11001, 1:200) in 1% antibody dilution buffer. Slides were then rinsed three times in 0.05% Tween-20 (Bio-Rad cat #170-0100)

in PBS and cover slipped using Slowfade Gold Antifade Reagent with DAPI (Invitrogen, cat # S36938) to counterstain cell nuclei.

### *Albumin*

Slides were washed three times in 0.1M PBS (pH 7.4), permeabilized with 0.1% Triton-X 100, then incubated for 2hr at room temperature with the primary antibody (FITC-conjugated goat anti-mouse Albumin, Bethyl Laboratories, cat # A90-234F, 1:200) in 1% antibody dilution buffer. Slides were then rinsed three times in 0.05% Tween-20 in PBS and cover slipped using Slowfade Gold Antifade Reagent with DAPI to counterstain cell nuclei.

### 2.5. *Imaging*

All imaging was performed using a Zeiss LSM 700 confocal laser scanning microscope, using a 40x oil objective, and in some instances zoom capture at 1.5x. Images were obtained using a fixed parameter setting to ensure consistency across images for qualitative analysis and comparison. The primary area of interest was upper and/or lower base at the mid-modiolar level, with particular focus on the cochlear lateral wall and capillaries of the stV. Specific regions of stV were re-imaged at 1.5x zoom for more detailed viewing of strial capillaries.

## **3. Results**

### 3.1 *Dispersion Patterns of Fluorescent beads*

The aim of the bead work was to probe possible capillary occlusion or abnormal capillary permeability in response to a single intense NE. This was achieved by perfusing the cochleae

with carboxylate-modified fluorescent microspheres. Cochlear vessels in the lateral wall, from stV or spLig, have approximately the same diameter, 6-10 $\mu$ m (Duvall et al., 1971). Bead size (0.02 $\mu$ m, 0.5 $\mu$ m) and delivery method were based on strial capillary diameter, and several trials using various bead sizes and previous work by Ohlemiller, Dwyer and Gagnon (2008, unpublished). The largest beads utilized did not show evidence of leakage into the pericapillary space or capillary occlusion (Fig. 8). Subsequent trials utilizing smaller bead sizes correlated with previous results (Figs. 9, 10, 11). That is, viewing at the mid-modiolar level did not evidence either occlusion or excessive permeability of capillaries regardless of bead size, control or noise-exposed conditions and mouse strain (Fig. 10). Both the larger and smaller beads were kept within the boundaries of, and evenly dispersed in the capillaries of CBA, CBA/J, BALB and B6 mice suggesting normal capillary anatomy and structural integrity, at least down to 20 nanometers. In addition, one trial utilized three bead sizes (compared to two) to assess the size of any apertures in the capillary walls, however results again supported previous trials (Fig. 12). This combination of three beads was not pursued, because adequate mixing of the beads during either the sonication process or transcardial perfusion could not be controlled for, which could compromise dispersion pattern, or cause capillary occlusion.

Spiral ligament was not observed to undergo pathological changes as evidenced by exclusion of or occlusion by fluorescent bead. However, vessels supplying the spLig and stV are largely independent (Axelsson and Ryan, 2001).



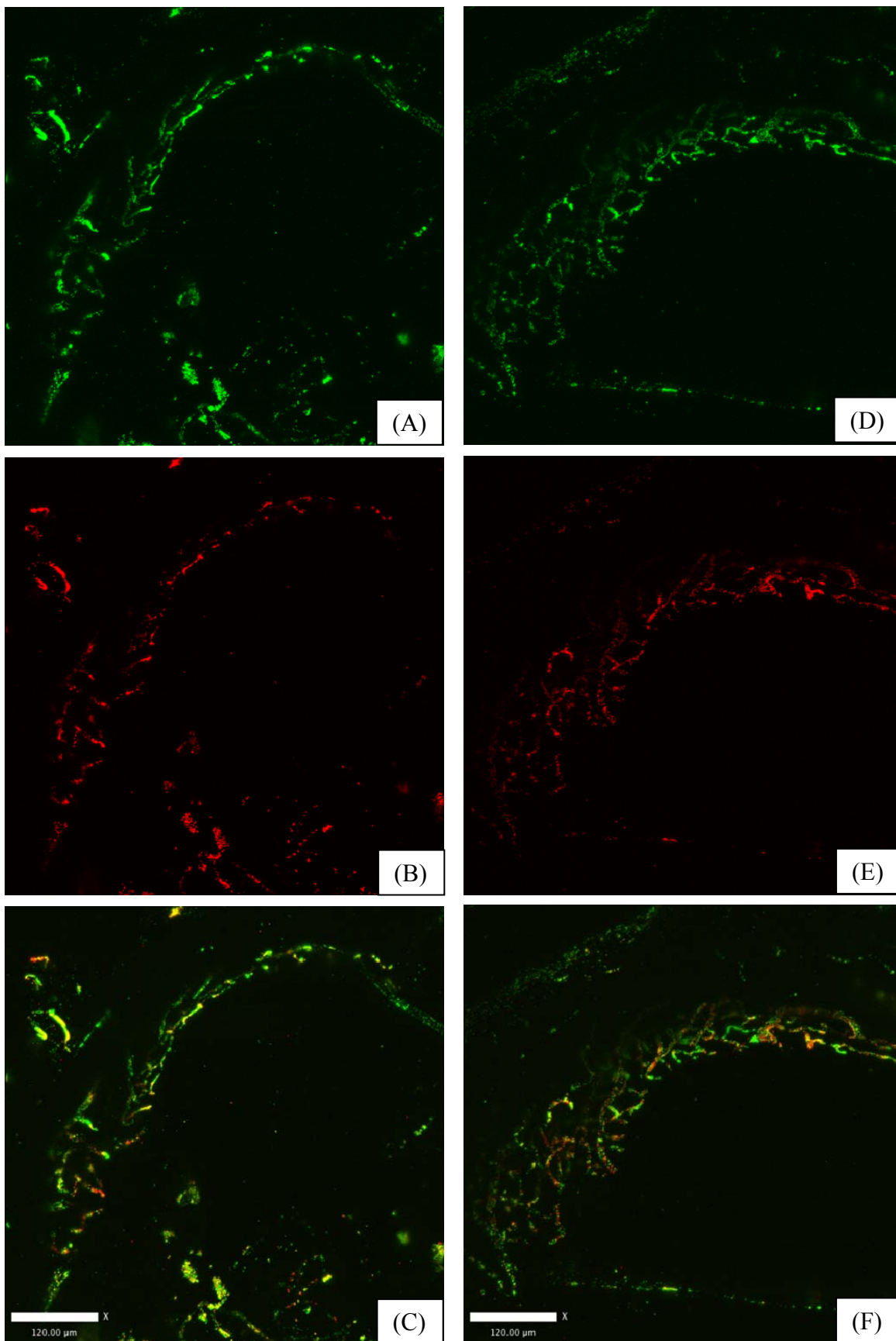


**Fig. 8** CBA/J control mice (A-C) and noise exposed (D-F) with 1.0 (red bead) and 0.5 $\mu$ m (green) beads at 1:1 dilution, imaged using a 20x objective; all images of strial upper base; CBA/J control and noise exposed mice evidenced intact capillary boundaries based on retention of the beads; and no evidence of bead dispersion into the pericapillary space was observed.

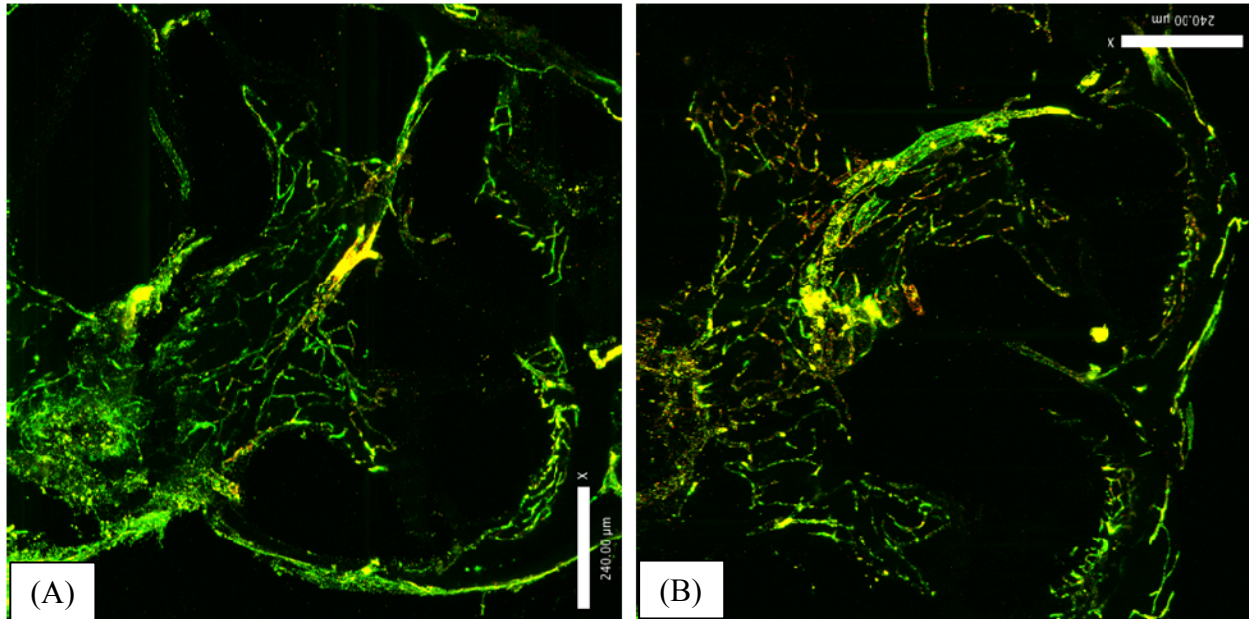


**Fig. 9** CBA/CaJ control mouse (A) and noise exposed (B) perfused with 0.5 and 0.2 $\mu$ m beads at a 1:1 dilution, imaged using a 10x objective, upper base. There was no evidence of either excessive leakage of the bead into pericapillary space or capillary occlusion.

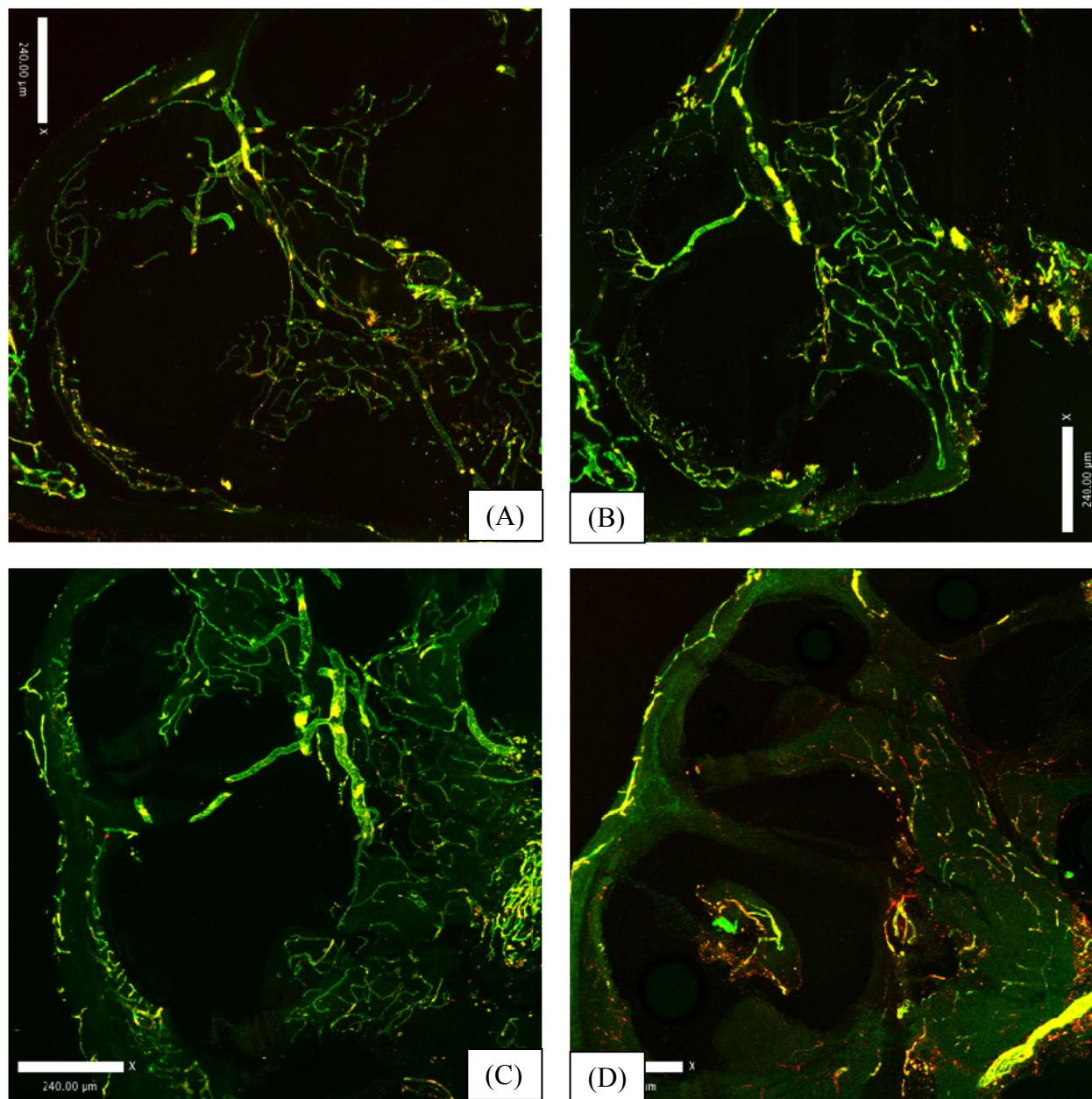


**Fig. 10** Composite images of 4 subjects perfused with  $0.5\mu\text{m}$  and  $0.02\mu\text{m}$  beads at a 1:1 dilution and captured using a 10x objective. (A) BALB control mouse; (B) BALB noise exposed mouse; (C) CBA/J control mouse; and (D) CBA/J noise exposed mouse. There was neither evidence of excessive leakage of the bead into pericapillary space nor capillary occlusion when using the smallest bead ( $0.02\mu\text{m}$ ) and the second to largest bead ( $0.5\mu\text{m}$ ).



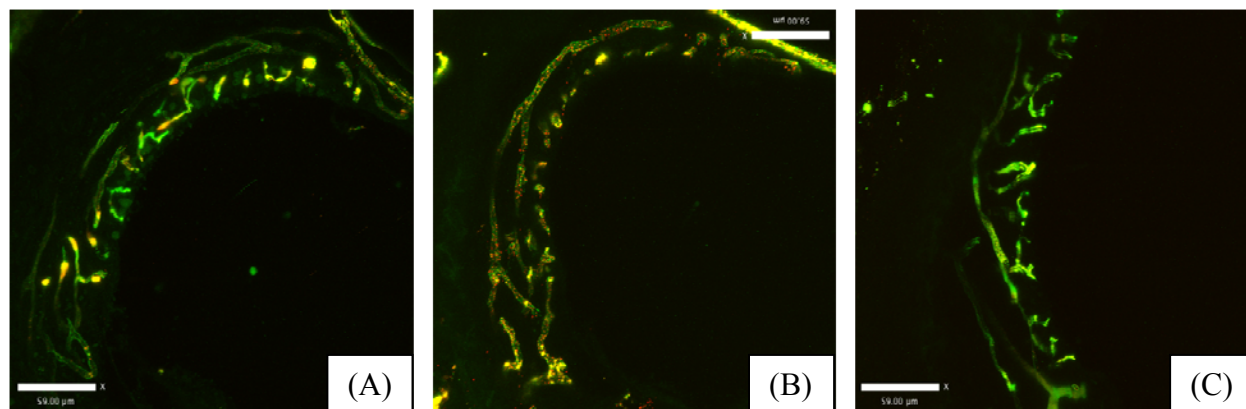


**Fig. 11** Upper basal stria captured at 40x of a B6 control mouse (A), B6 noise exposed mouse (B) and a CBA control mouse (C), all perfused with 0.2 and 0.02  $\mu\text{m}$  beads. Again, these images correlate to previous results in that they do not demonstrate disruption of capillary vessels, evidenced by leakage or occlusion in both control and noise exposed subjects, regardless of strain and using the two smallest bead sizes.

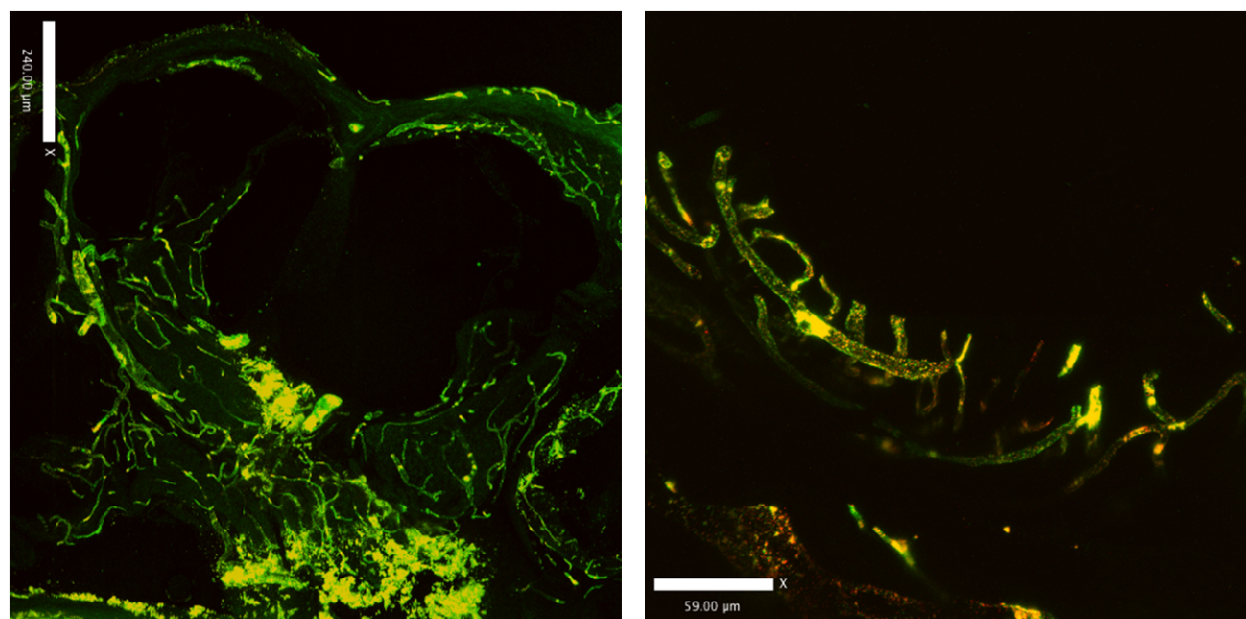


**Fig. 12** CBA/CaJ control mouse perfused with three beads, 1.0, 0.2 and 0.02  $\mu\text{m}$  beads. (A) Shows a mid-modiolar view of the upper basal turn of the cochlea, using a 10x objective. (B) Shows a magnified (40x) view of the strial capillaries in the upper base (in a different subject). Although the three beads were observed to disperse evenly, the possibility of occlusion due to inadequate bead mixing (during sonication or transcardial perfusion) prevented further trials using three beads instead of two.

### 3.2. *Immunohistochemistry*

To support findings from the fluorescent bead (capillary leakage) portion of the study immunohistochemistry was performed probing for two antibodies (albumin, IgG). Previously thought to be immune-privileged due to the blood-labyrinth barrier (similar to the brain), IgG has been shown to naturally reside in the cochlea, though at levels as low as 1/1000<sup>th</sup> compared to serum in the rest of the body (Quintana and Cohen, 2004; Harris and Ryan, 1995). Albumin is the primary protein constituent in blood plasma and serum.

#### *IgG*

Strain differences were observed for BALB and B6 mice, which demonstrated excessive leakage, i.e. staining of IgG, compared to CBA/CaJ mice for both control and noise exposed conditions (Figs. 13, 15b, 16b). Condition differences, i.e. whether animals were noise exposed, did not appear to affect overall staining pattern in CBA mice (Fig.14). B6 and BALB mice showed IgG dispersion into the pericapillary space in both conditions (Figs.15a, 16a), which was particularly evident in images of the capillary bed, captured using a 60x objective (Figs. 15b, 16b). However, B6 and BALB mice did reveal qualitative changes in the degree of staining in the control versus noise exposed conditions, suggesting a noise-mediated response (Figs. 15, 16). From a strictly *strain* dependent view IgG staining was present in B6 control animals and to a lesser extent in BALB control mice but not in CBA control mice. Qualitative analysis of IgG staining in their noise counterparts demonstrated slight increases in the degree of staining for B6 and BALB mice, but little change in CBA mice. Taken as a whole, these results suggest excessive permeability of capillaries, illustrated by leakage of IgG in the pericapillary space, may not affect the EP.

*Albumin*

Albumin proved a difficult antibody to use because of the amount of background staining, despite several dilution series. This does not necessarily preclude the use of albumin as a reliable antibody as previous work has demonstrated its successful application (Cohen-Salmon et al., 2007), but results from this study do indicate the need for further investigation.

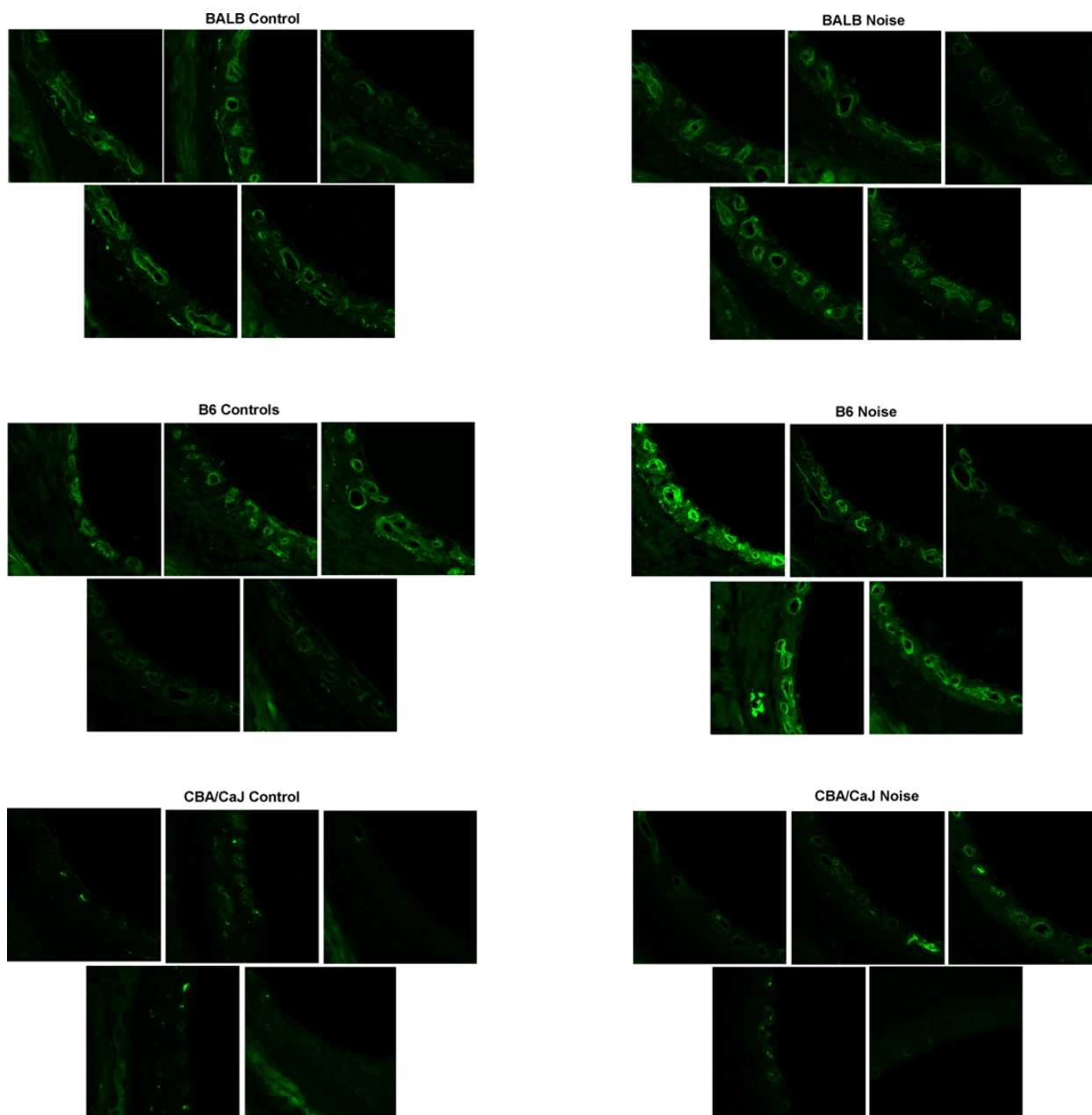


**Fig. 13** Overall IgG results separated by strain and condition; images captured using a 40x objective. Strain differences can be seen in BALB and B6 control mice, which exhibit excessive IgG staining when compared to CBA mice for both control and noise exposed conditions.

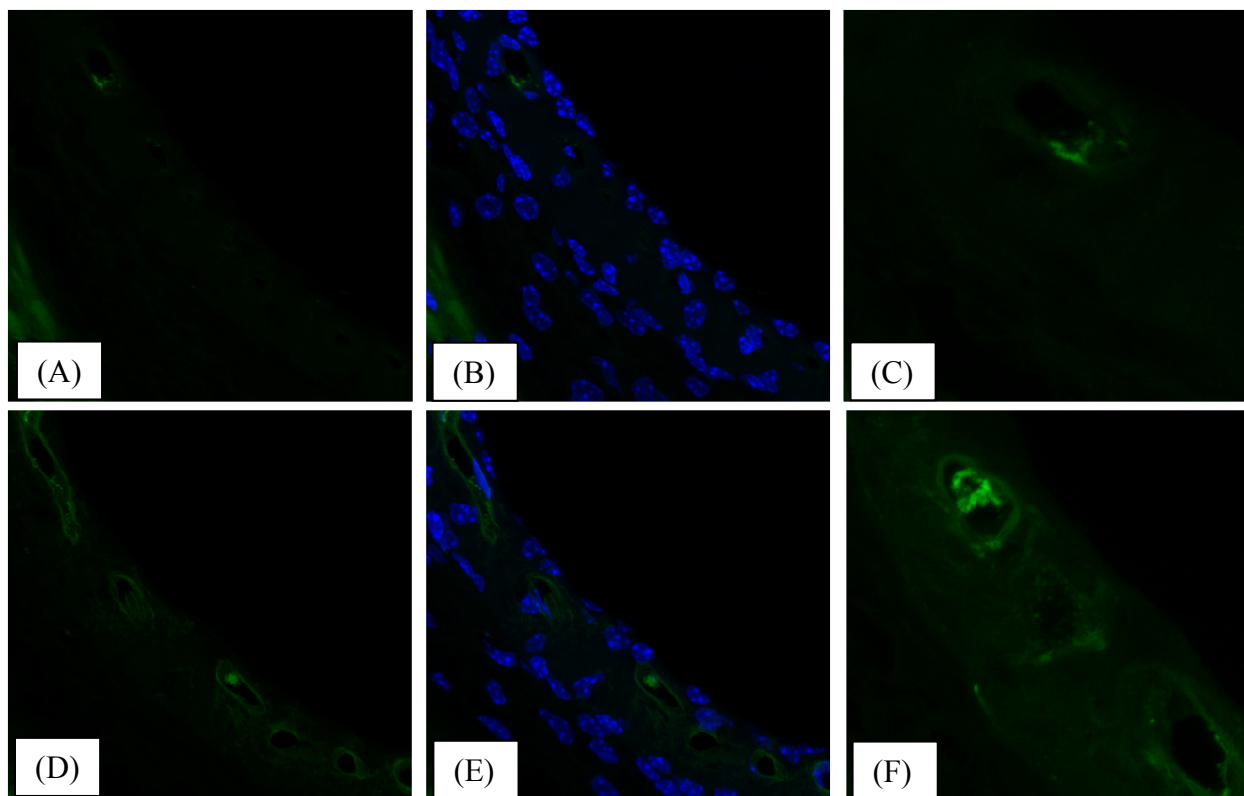


**Fig. 14** CBA/CaJ control (A-C) and noise exposed (D-F) mice stained with IgG. 40x objective images (A, B, D, E) without DAPI staining (A, D) and with DAPI (B, E) demonstrate no significant differences in staining pattern, that is noise exposure did not induce excessive capillary permeability. 60x objective images (C, F) provide a magnified image of the capillary bed and like their 40x counterparts do not demonstrate staining in the pericapillary space. The bright cluster of staining in (F) is likely remaining red blood cells in the capillary lumen.

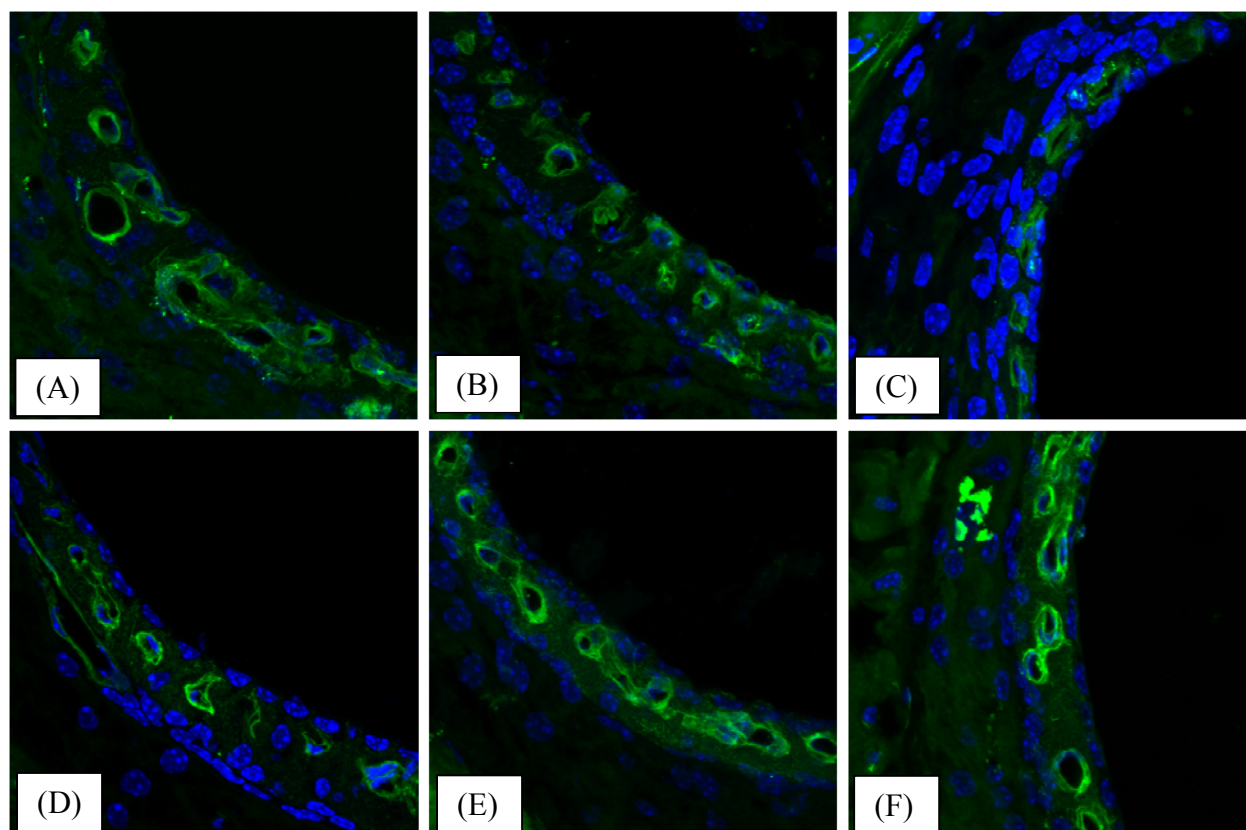


**Fig. 15a** B6 control (A-C) and noise exposed (D-F) mice; images of the upper base, captured at 40x. Gross qualitative analysis revealed slight increases in the degree of IgG staining, particularly comparing (B) and (E) and (C) and (F).



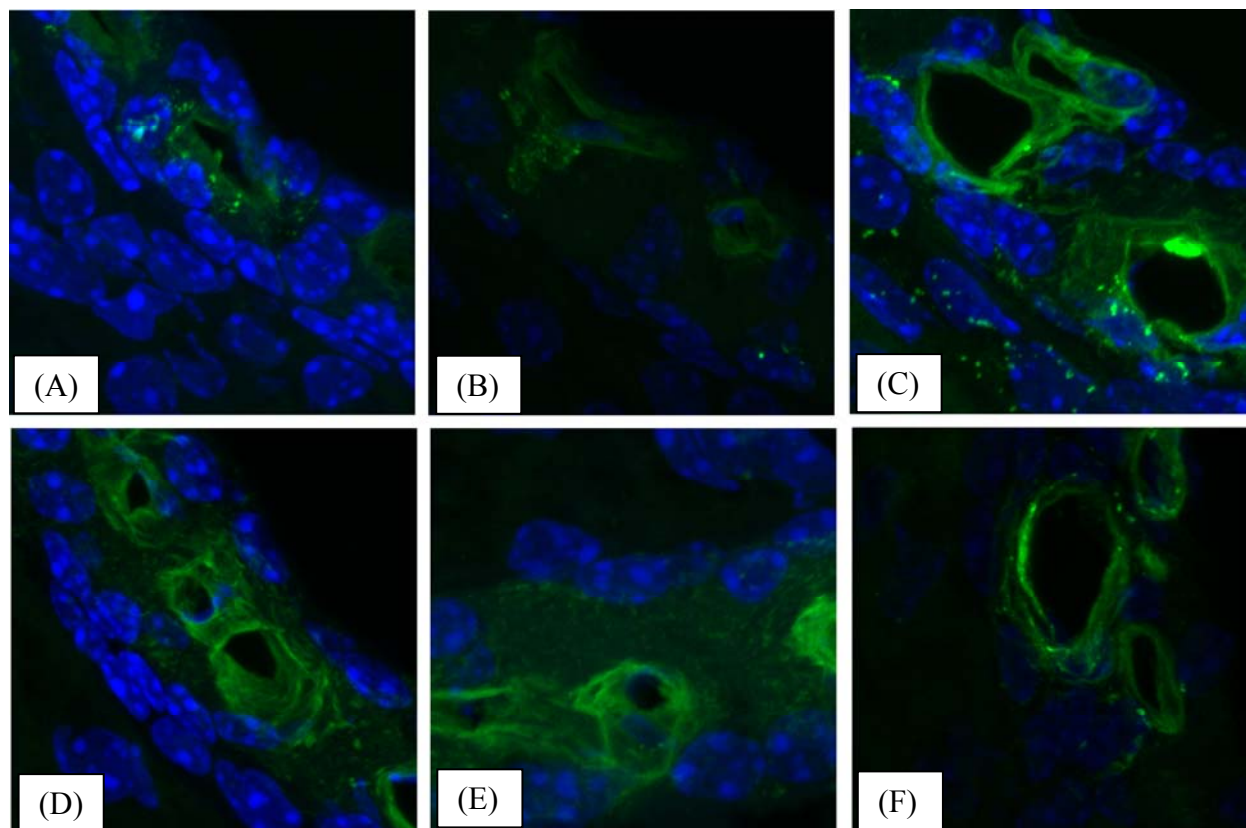


**Fig. 15b** B6 control (A-C) and noise exposed (D-F) mice; images of the strial capillary bed, captured at 60x. Qualitative analysis revealed observable increases in the degree of IgG staining when comparing control versus noise exposed mice. Condition independent, this higher magnification was intended to elucidate more clearly where the staining was in relation to capillaries, pericytes and the basal laminae. The punctate pattern observed in the pericapillary spaces suggests leakage rather than background effects.

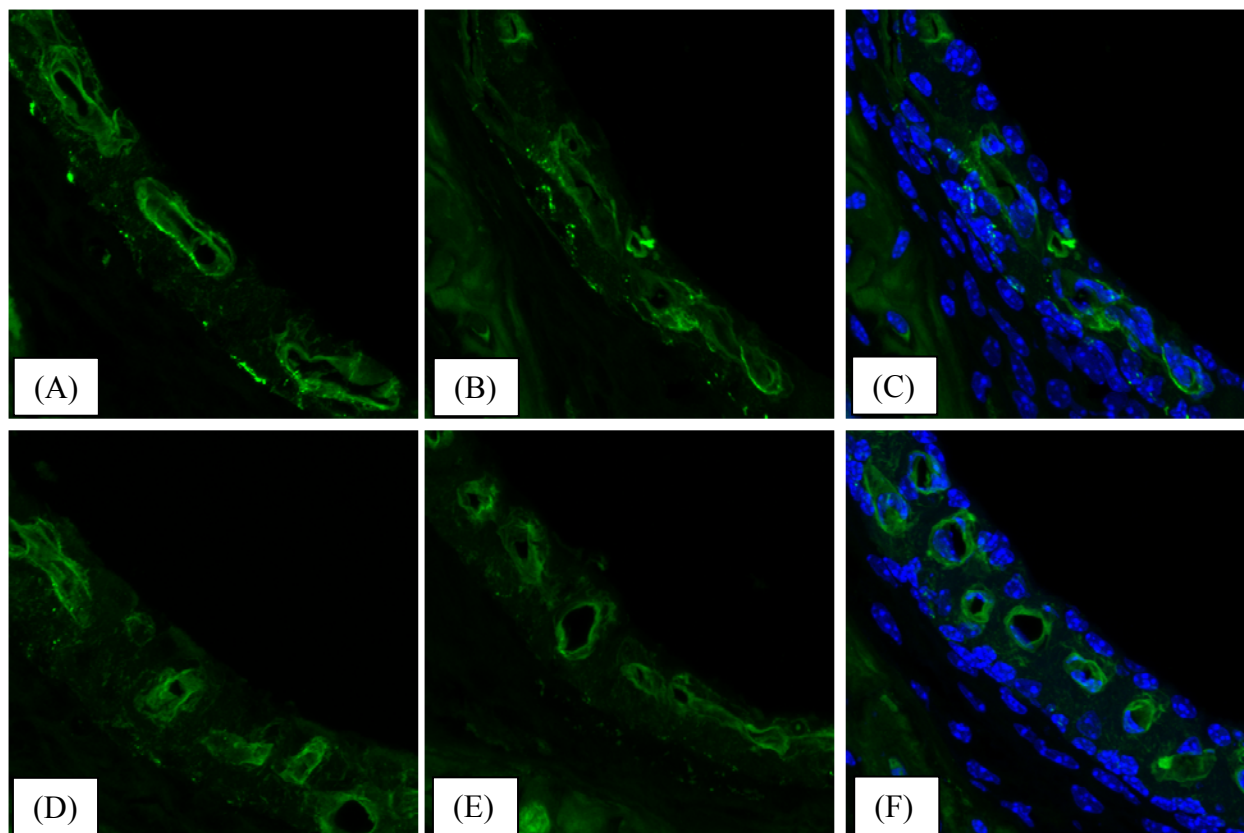


**Fig. 16a BALB** control (A-C) and noise exposed (D-F) mice, images captured using a 40x objective either with DAPI (C, F) or without (B, E). IgG is present in both conditions as evidenced by the punctate staining in the pericapillary space, with slight increases in amount of staining in the noise exposed animals (e.g. (D)).

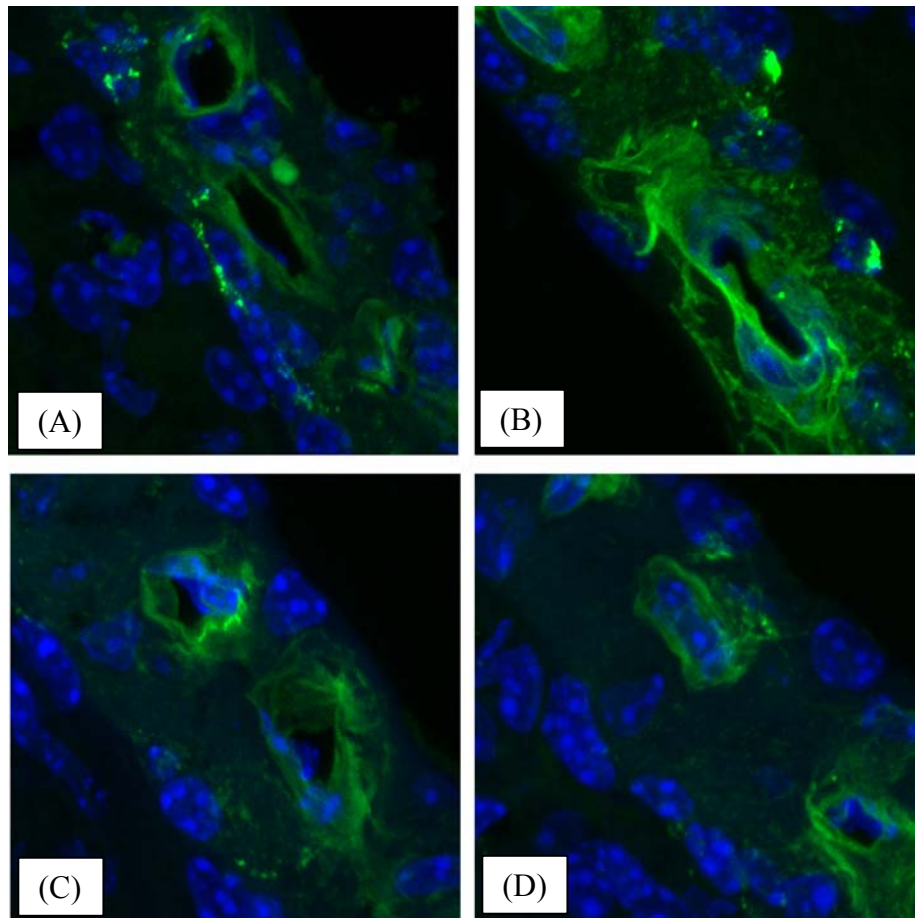


**Fig. 16b** BALB control (A, B) and noise exposed (C, D) mice imaged at 60x. IgG staining was present in both conditions and can be seen in the pericapillary space, surrounding pericytes and gathering in the vicinity of the basal laminae.

#### 4. Discussion

Recent experiments in mice have shown that noise exposure can reduce the EP even when the gross appearance of the stria vascularis is fairly normal (Hirose and Liberman, 2003; Ohlemiller, 2007). The mechanism responsible for this reduction has not been established. Alteration of strial capillaries, in the form of excessive permeability or occlusion, is a possibility. The purpose of this study was to probe capillary endothelial cell integrity in mice that either do, or do not exhibit loss or reduced EP following a single intense noise exposure. Two methods were applied: perfusion with fluorescent microspheres and immunohistochemistry using IgG and albumin.

#### 4.1. *Fluorescent Microspheres*

Transcardial perfusion of fluorescent beads did not yield results consistent with either excessive leakage or capillary occlusion in mice in response to noise. From our results, we tentatively rule out that noise causes EP reduction by promoting large, uncontrolled openings between strial capillary endothelial cells that allow  $K^+$  and other small ions to equilibrate across strial capillary walls. However, the smallest bead size applied (20 nanometers) is approximately 10 times the size of a potassium ion. Thus small fenestrations just sufficient to allow ion would not have been detected. Subsequently, probing for holes smaller than 20 nanometers, small enough to let  $K^+$  ions pass, will require further trials utilizing either smaller beads, or a different tracer. Pilot experiments using FITC-Dextran and either intraperitoneal or tail vein injection delivery showed shortcomings, particularly limitation of permissible volume fluid injection (Ohlemiller, Dwyer and Gagnon, unpublished).

#### 4.2. *Immunohistochemistry*

The different IgG staining patterns observed in CBA, BALB and B6 mice suggest that passage of IgG into the putatively immuno-privileged intrastrial space is more complex than has been thought. First, there was a significantly reduced amount of IgG staining in CBA noise exposed mice, a strain known to exhibit a reduced EP following noise exposure. Second, robust IgG staining was seen in B6 noise exposed mice, yet this strain has been shown to be resistant to EP reduction following noise exposure. While results were not quantified, these findings undermine any simple interpretation of uncontrolled capillary leak as a mechanism of EP reduction. The pericapillary leakage observed in B6 and BALB mice regardless of condition points to the larger question of controlled or uncontrolled dispersion of IgG. That is, is the

leakage evidenced by IgG staining an adaptive process or something unregulated? Controlled or regulated permeability has been demonstrated in early work by Duvall (1971) and others. Their studies investigated normal capillary permeability using horseradish peroxidase (HRP) and found regulated micropinocytotic uptake of the tracer (Duvall and Klinker, 1983; Sakagami et al., 1982). In contrast, Hukee and Duvall (1985) suggest normal animals do not demonstrate breach of capillary integrity as evidenced by HRP leakage. In either case, HRP can induce a histamine response, triggering pinocytosis and resulting in leaky vessels, which raises the question of whether live animals are appropriate subjects. Sakagami and colleagues (1982) found less dispersion of HRP when injected in dead rather than live animals. Their results indicate that dead animals should be used to prevent the continuation of active processes.

Yet, what could not be determined was whether HRP was actively transported across endothelial cell boundaries or if it represented uncontrolled leakage. Building on this early work, more recent research has shown uncontrolled leakage under different conditions and tracers: Shi (2007) found extrusion of IgG into pericapillary space following acoustic trauma; Cohen-Salmon et al. (2007) demonstrated leakage of IgG and albumin in the intrastrial space in Cx30 knockout mice; and Lin and Trune (1997) found breakdown of the blood-labyrinth barrier in autoimmune disease mice using ferritin.

While it could be argued that results in this study might be artifact (i.e. background staining of IgG), two primary observations quell this notion: (1) there was a striking absence of IgG in CBA mice and (2) other cochlear tissue did not show staining, e.g. spiral limbus, spiral ligament and the tectorial membrane.

Results from this study offer confounding data as IgG staining was evident in control animals (BALB and B6), suggesting that it may be normally present in the stria vascularis. Further, pathologic leakage, e.g. caused by intense noise exposure, increases capillary permeability (Hukee and Duvall, 1985), therefore the differences observed in the degree of IgG dispersion in BALB and B6 noise exposed mice may point to an adaptive process, whereby this antibody is actively taken up by cells surrounding the capillary. Consequently, present results offer a novel phenomenon that has not been previously demonstrated, which could challenge earlier findings, and future research is called for.

## REFERENCES

- Ahmad, M., Bohne, B., Harding, G. (2003). An in vivo tracer study of noise-induced damage to the reticular lamina. *Hearing Research*, 175, 82-100.
- Axelsson, A., Ryan, A. (2001). Circulation of the Inner Ear: I. Comparative Study of the Vascular Anatomy in the Mammalian Cochlea. In A.F. Jahn & J. Santos-Sacchi (Eds.) *Physiology of the Ear* (2<sup>nd</sup> ed.), (p307). Canada: Singular Thomson Learning.
- Clark, W. (2008). Basic Acoustics and Noise. In W.W. Clark & K.K. Ohlemiller (Eds.) *Anatomy and Physiology of Hearing for Audiologists* (pp. 16 -17). Clifton Park, NY: Thomson Delmar Learning.
- Cohen-Salmon, M., Regnault, B., Cayet, N., Caille, N., Demuth, K., Hardelin, J., Janel, N., Meda, P., Petit, C. (2007). Connexin30 deficiency causes intrastrial fluid-blood barrier disruption within the cochlear stria vascularis. *Proceedings of the National Academy of Sciences*, 104(15), 6229-6234.
- Duvall, A., Klinker, A. (1983). Macromolecular tracers in the mammalian cochlea. *American Journal of Otolaryngology*, 4(6), 400-410.
- Duvall, A., Quick, C., Sutherland, C. (1971). Horseradish peroxidase in the lateral cochlear wall. *Archives of Otolaryngology*, 93, 304-316.
- Gelfand, S. (2007). *Hearing an Introduction to Psychological and Physiological Acoustics* (4<sup>th</sup> ed.), p137. New York: Informa Health Care.
- Harris, J., Ryan, A. (1995). Fundamental immune mechanisms of the brain and inner ear. *Otolaryngology Head and Neck Surgery*, 112(6), 639-653.
- Hibino, H., Kurachi, Y. (2006). Molecular and physiological bases of the k<sup>+</sup> circulation in the mammalian inner ear. *Physiology*, 21, 336-345.
- Hirose, K., Liberman, MC. (2003). Lateral wall histopathology and endocochlear potential in the noise-damaged mouse cochlea. *Journal of the Association for Research in Otolaryngology*, 4, 339-352.
- Hirose, K., Discolo, C., Keasler, J., Ransohoff, R. (2005). Mononuclear phagocytes migrate into the murine cochlea after acoustic trauma. *The Journal of Comparative Neurology*, 489, 180-194.
- Hudspeth, A., Choe, Y., Mehta, A., Martin, P. (2000). Putting ion channels to work: mechano-electrical transduction, adaptation and amplification by hair cells. *Proceedings of the National Academy of Sciences*, 97(22), 11765-11772.

- Hukee, M., Duvall, A. (1985). Cochlear vessel permeability to horseradish peroxidase in the normal and acoustically traumatized chinchilla: a reevaluation. *Annals of Otolaryngology, Rhinology and Laryngology*, 94, 297-303.
- Kwan, K., Allchorne, A., Vollrath, M., Christensen, A., Zhang, D., Woolf, C., Corey, D. (2006). TRPA1 contributes to cold, mechanical and chemical nociception but is not essential for hair-cell transduction. *Neuron*, 50, 277-289.
- Lin, D., Trune, D. (1997). Breakdown of stria vascularis blood-labyrinth barrier in C3H/lpr autoimmune disease mice. *Otolaryngology Head and Neck Surgery*, 117(5), 530-534.
- Nin, F., Hibino, H., Doi, K., Suzuki, T., Hisa, Y., Kurachi, Y. (2008). The endocochlear potential depends on two K<sup>+</sup> diffusion potentials and an electrical barrier in the stria vascularis of the inner ear. *Proceedings of the National Academy of Sciences*, 105(5), 1751-1756.
- Ohlemiller, K. (2002). Reduction in sharpness of frequency tuning but not endocochlear potential in aging and noise-exposed BALB/cJ mice. *Journal of the Association for Research in Otolaryngology*, 3, 444-456.
- Ohlemiller, K., Gagnon, P. (2007). Genetic dependence of cochlear cells and structures injured by noise. *Hearing Research*, 224, 34-50.
- Ohlemiller, K., Rybak Rice, M., Gagnon, P. (2008). Strial microvascular pathology and age-associated endocochlear potential decline in NOD congenic mice. *Hearing Research*, 244, 85-97.
- Ohlemiller, K., Wright, J., Heidbreder, A. (2000). Vulnerability to noise-induced hearing loss in 'middle-aged' and young adult mice: a dose-response approach in CBA, C57BL, and BALB inbred strains. *Hearing Research*, 149, 239-247.
- Ohmori, H. (1992). Ion channels for the mechano-electrical transduction and efferent synapse of the hair cell. *Advances in Biophysics*, 28, 1-30.
- Quintana, F., Cohen, I. (2004). The natural autoantibody repertoire and autoimmune disease. *Biomedicine and Pharmacotherapy*, 58, 276-281.
- Robles, L., Ruggero, M. (2001). Mechanics of the mammalian cochlea. *Physiological Reviews*, 81(3), 1305-1352.
- Sakagami, M., Matsunaga, T., Hashimoto, P. (1982). Fine structure and permeability of capillaries in the stria vascularis and spiral ligament of the inner ear of the guinea pig. *Cell and Tissue Research*, 226, 511-522.
- Schulte, B., Schmiedt, R. (1992). Lateral wall Na, K-ATPase and endocochlear



- potentials decline with age in quiet-reared gerbils. *Hearing Research*, 61, 35-46.
- Shi, X. (2009). Cochlear pericyte responses to acoustic trauma and the involvement of HIF-1 $\alpha$  and VEGF. *The American Journal of Pathology*, 174(5), 1692-1704.
- Suzuki, M., Yamasoba, T., Kaga, K. (1998). Development of the blood-labyrinth barrier in the rat. *Hearing Research*, 116, 107-112.
- Takeuchi, S., Ando, M., Sato, T., Kakigi, A. (2001). Three-dimensional and ultrastructural relationships between intermediate cells and capillaries in the gerbil stria vascularis. *Hearing Research*, 155, 103-112.
- Trune, D. (1997). Cochlear immunoglobulin in the C3H/*lpr* mouse model for autoimmune hearing loss. *Otolaryngology Head and Neck Surgery*, 117(5), 504-508.
- Wang, Y., Hirose, K., Liberman, MC. (2002). Dynamics of noise-induced cellular injury and repair in the mouse cochlea. *Journal of the Association for Research in Otolaryngology*, 3, 248-268.
- Wangemann, P. (2002). K<sup>+</sup> cycling and the endocochlear potential. *Hearing Research*, 165(1-2), 1-9.
- Wangemann, P. (2006). Supporting sensory transduction: cochlear fluid homeostasis and the endocochlear potential. *Journal of Physiology*, 576(1), 11-21.
- Whitlon, D., Szakaly, R., Greiner, M. (2001). Protocol: cryoembedding and sectioning of cochleas for immunohistochemistry and in situ hybridization. *Brain Research Protocols*, 6, 159-166.
- Yost, W. *Fundamentals of Hearing* (4<sup>th</sup> ed.), p 106. San Diego, CA: Academic Press.